Supporting Information

Three-Dimensional Visualization of Conductive Domains in Battery Electrodes with Contrast-Enhancing Nanoparticles

*Samantha L. Morelly[1], Jeff Gelb[2], Francesco Iacoviello[3], Paul R. Shearing[3], Stephen J. Harris[4], Nicolas J. Alvarez[1], *Maureen H. Tang[1]*

1. Department of Chemical and Biological Engineering, Drexel University, Philadelphia, PA 19104, USA

2. Carl Zeiss X-Ray Microscopy, 4385 Hopyard Rd. Ste. 100, Pleasanton, CA 94588

3. Electrochemical Innovation Lab, Department of Chemical Engineering, University College London, London WC1E 7JE, United Kingdom

4. Materials Science Division, Lawrence Berkeley National Lab, Berkeley, CA 94720

*mhtang@drexel.edu

Materials and Methods

Electrode fabrication and testing. Electrodes were made using MCMB graphite (MTI), $Ni_{0.33}Mn_{0.33}Co_{0.33}O_2$ (NM-3100, TODA America, Battle Creek, MI) , polyvinylidene difluoride (PVDF) (Ky301F, MW = 380k) (Arkema, King of Prussia, PA) and C-coated Fe nanoparticles (Fe-C, Millipore Sigma) with a mean particle size of 25 nm. The slurry was processed with 1-Methyl-2pyrrolidinone (NMP) (Millipore Sigma, ≥99%) as the solvent. Specific compositions and processing parameters are given in Table S1. Slurries were made by first dissolving PVDF in NMP at 1800 rpm in a Thinky planetary mixer until the PVDF was fully dissolved, then the desired particles were added to the PVDF/NMP solution and mixed at 1800 rpm in the Thinky for 7.5 minutes. The resulting slurries were coated onto a copper current collector and dried using as specified in Table S1.

Due to the density difference between carbon black and Fe-C, additional electrodes with higher conductive additive content were fabricated for coin cell testing (Table S1). Sections of the dried electrode film were calendered to ~35% porosity with a rolling mill. 3/8" in diameter electrodes were then punched, dried at 100C for 1 hour, and transferred into an Ar glovebox. 2032 coin cells were assembled with ½" Li metal counter electrodes (Alfa Aesar). Coin cells were then tested on an Arbin battery cycler using a CC discharge and CC/CV charge at C/10.

Microscopy. Samples were prepared for SEM/EDS (Zeiss Supra 50VP, Thornwood NY / Oxford Instruments, Concord MA) by carefully cutting with a Personna double sided razor blade and mounting on 90-degree studs with carbon tape. A comparison of samples sliced top-down and bottom-up found no evidence of smearing binder or carbon through the sample. General SEM images were taken at 10kV and EDS measurements were taken at 19kV to insure sufficient voltage for Fe visibility.

XCT: Samples for nano-XCT were prepared from bulk foils by making crossed incisions with a razor blade and then mounting the small wedges to steel pins with adhesive. The Cu current collectors were removed in the region of interest by carefully peeling back the foil near the tip, where the specimen naturally began to delaminate. Each sample was inspected after preparation using an optical microscope (Zeiss Stemi 305, Thornwood NY), where the electrode layers were observed to still be planar and undisturbed by preparation. Finally, the pin-mounted samples were loaded into the pin-vise sample holder and installed into the nano-XCT (Zeiss 810 Ultra, Pleasanton CA).

In collecting the radiograph series for tomography, 901 images were collected across a rotation angle range of 180°, exposing each image for 10 seconds. This resulted in a total acquisition time of ~3 hours, using an effective pixel size of 126 nm. The radiograph series was subsequently reconstructed using a filtered back projection reconstruction algorithm (Zeiss XMReconstructor, Pleasanton, CA), producing a 3D volume suitable for subsequent analysis.

Image analysis: Three different samples were analyzed with the nano-XCT technique: graphite-PVDF, Fe-PVDF, and graphite-Fe-PVDF. Each of the three specimens was trimmed to the same size and shape, and 3D reconstructions were performed using identical scaling parameters. Thus, a relative CT scaling was achieved between samples, allowing direct comparison of the CT numbers between datasets. Using this procedure, the CT number ranges for Fe, graphite, and PVDF + pore were uniquely determined, providing high confidence in the resulting numerical analysis.

The Fe-PVDF dataset was analyzed first, where the difference between Fe and PVDF could be clearly determined through visual inspection of the greyscale histograms. A simple thresholding procedure was used to determine the range of CT numbers corresponding to Fe, applied using the Fiji distribution of the ImageJ software (National Institute of Health, Bethesda, MD). In the simple thresholding procedure, an upper and lower bound are set for a dataset, where all greyscale values between these bounds are assigned to a particular material. This found a lower threshold range between 2300-2600, which led to a CT number range determination of [2300, MAX] or [2600, MAX], with the difference between 2300 and 2600 quantifying inherent errors in the measurement. A threshold of 2300 calculated a CBD volume fraction of 1.2%, while the threshold at 2600 found the CBD volume fraction to be 0.7 vol%. In a second step, a similar procedure was applied to the graphite-PVDF dataset, which resulted a lower greyscale threshold of 600 for the graphite particles. Thus, a CT number range of [600, 2300) or [600, 2600) was determined for graphite. Finally, the found threshold ranges were applied to the graphite-Fe-PVDF dataset as [MIN, 600) for pore+PVDF, [600, 2300-2600) for graphite, and [2300-2600, MAX] for Fe. Results were tabulated for both Fe threshold levels, in order to compare to the known quantities of material used to prepare the specimen. Further quantitative analysis of Fe clusters and material distributions were performed with Fiji, and 3D visualization was achieved using the Tomviz software package (Kitware, Inc., Clifton Park, NY) and Avizo 9.4 (Thermo Fisher Scientific, Hillsboro, USA).

Table S1: Compositions and fabrication parameters for electrodes in this study

Sample	Graphite (wt%)	Fe-C (wt%)	PVDF (wt%)	Coating thickness (wet)	Drying parameters
(EDS-1) Graphite-Fe-PVDF	95	2.5	2.5	200 µm	2 hours, 80C
(EDS-2) Graphite-Fe-PVDF	95	2.5	2.5	200 µm	2 hours 25C + 16 hours, 80C

(XCT-1) Graphite-PVDF	97.4	0	2.6	100 µm	16 hours, 25C
(XCT-2) Fe-PVDF	0	33	67	100 µm	16 hours, 25C
(XCT-3) Graphite-Fe-PVDF	95	2.5	2.5	100 µm	16 hours, 25C
(BATT-1) Graphite-Fe-PVDF	78	10	12	100 µm	18 hours, 70 C + 12 hours, 120C (vacuum)
(BATT-2) NMC-Fe-PVDF	78	10	12	100 µm	16 hours, 25 C + 12 hours, 120 C (vacuum)

Electrochemical and processing behavior of carbon black vs. Fe-C

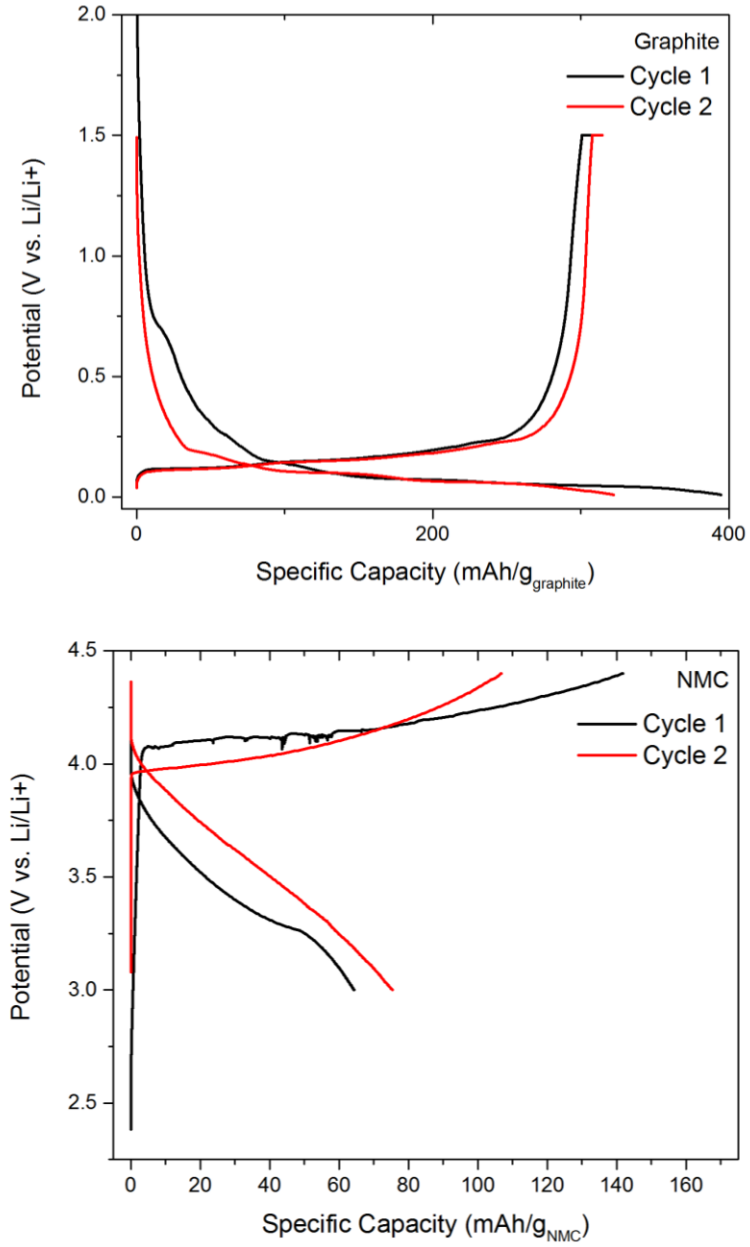

Figure S1: Electrode charge/discharge profiles for Graphite - Fe - PVDF at C/10 rate (top) and NMC - Fe - PVDF (bottom) at C/10 rate.

Battery discharge curves in Figure S1 show that graphite electrodes with Fe-C as conductive additive can reach approximately the theoretical capacity of graphite if the volume fraction of conductive additive is sufficient. The Fe-C was also tested as a conductive additive for

$Ni_{0.33}Mn_{0.33}Co_{0.33}O_2$, (NMC), a common cathode material. In this case, the Fe-C did not function as a conductive additive. The charging curve is characterized by a plateau at 4.1 V instead of the characteristic profile of NMC, and the discharge voltage falls steeply. This behavior is consistent with Fe oxidation followed by dissolution of the conductive additive and formation of insulating side reaction products. Although such undesirable Fe oxidation may be mitigated by minimizing defects in the carbon coating of the Fe-C nanoparticles, Figure S1 shows that commercially available Fe-C is not suitable as a conductive additive at high potential. Al is stable at oxidizing potentials in Li-ion electrolytes and may be a suitable substitute for Fe-C.

For Fe-C to perform effectively as a diagnostic tool for electrode microstructure, it should behave similarly to carbon additive in electrode processing. Adequate processing is essential for optimal electrode performance. Above the critical volume fraction, the colloidal properties of carbon black stabilize electrode slurries via formation of a colloidal gel. For Fe-C to have the same colloidal behavior, it must have a similar gravitational Peclet number, which is the ratio between the Brownian diffusion time (τ_b) and gravitational settling time (τ_s) as seen in Equation S1.

$$Pe_g = \frac{\tau_b}{\tau_s} \sim \frac{2\pi\Delta\rho g a^4}{9k_BT}\left(\frac{R}{a}\right)^{d_f+1} \quad [S1]$$

$\Delta\rho$ is the difference between the density of the particles and the density of the solvent, a is the radius of the particles, R is the fractal cluster size, and d_f is the fractal dimension of the particle. If $Pe_g > 10$, then the gravitational settling time is an order of magnitude faster than the Brownian diffusion. For a typical carbon additive in NMP, $\Delta\rho = 0.872$ g/cm^3 and $a = 0.05$ microns, so R can be as large as 0.5 microns before gravitational forces cause settling and prevent beneficial slurry properties.

According to the manufacturer's product information, the average particle diameter of the Fe-C nanoparticles is 25 nm. Considering this smaller primary particle size, Fe-C fractal cluster sizes below ~1.4 microns should remain Brownian and resist settling, despite the higher density. However, large aggregates of particles could be observed visually in the powder, and suspensions of Fe-C in NMP settled immediately. This occurred despite efforts to avoid exposure to ambient water vapor, which often induces nanoparticle agglomeration. The agglomeration was mitigated by sonicating suspensions of Fe-C before adding PVDF and active material. The largest aggregates did not suspend, but smaller particles were stably suspended. No visible aggregates formed from the sonicated solution for at least ten minutes, before which the remaining slurry components were added and mixed. Further improvement in Fe-C suspension could likely be achieved by initial filtering of large aggregates before sonication or mixing.

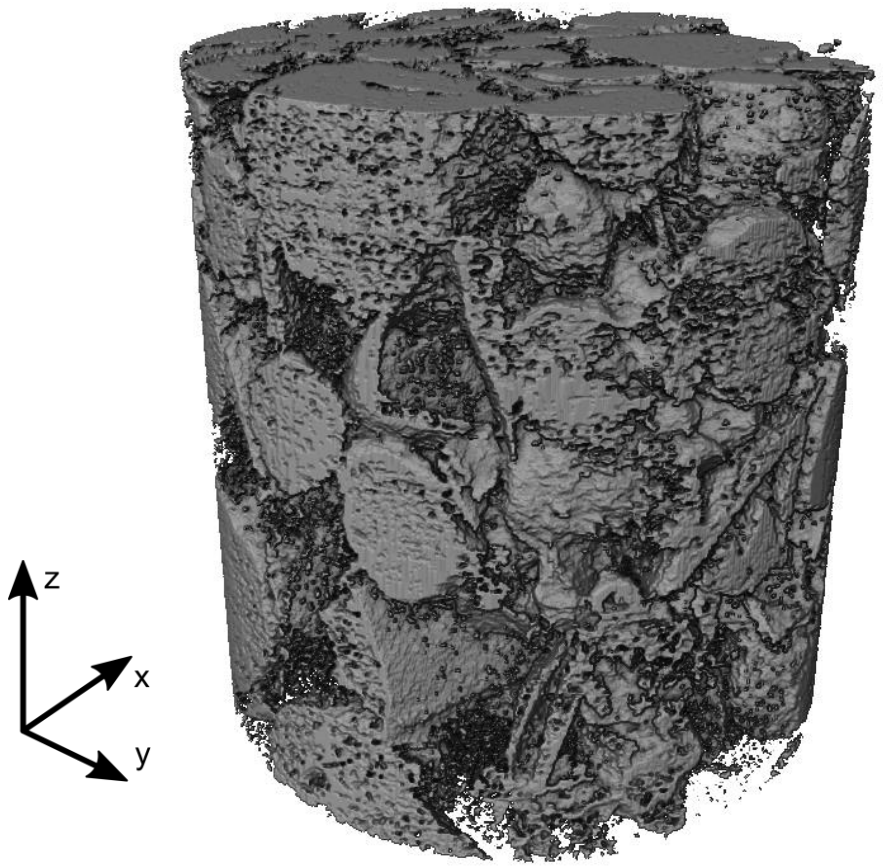

Figure S2: 3-D XCT rendering of graphite-PVDF electrode. The imaged cylinder is 65 µm in diameter.

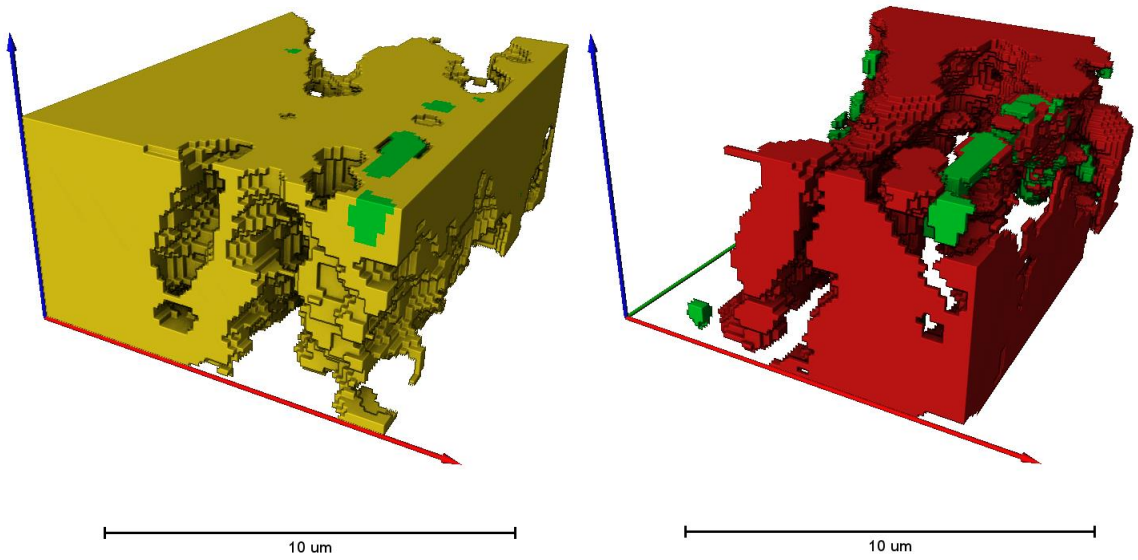

Figure S3: Sub-volume renderings of graphite (yellow), CBD (green), and void (red) to show connectivity of particles. Volume fractions are 63.6%, 1.7%, and 34.7%, respectively. Voxels sharing at least one common vertex are considered connected.

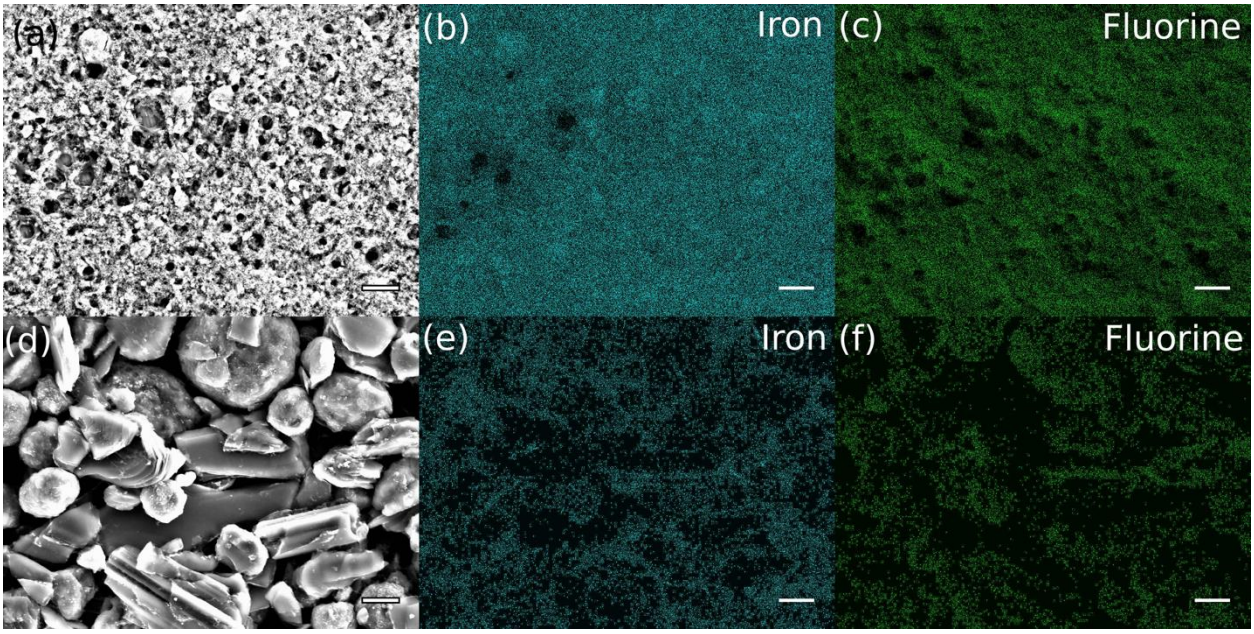

Figure S4: SEM and EDS maps for the surface of XCT-2 (a-c) and XCT-3 (d-f) prepared graphite electrodes with Fe contrast-enhancing agent. For each image, the scale bar corresponds to 10 microns. (a, d) SEM images (b, e) Fe EDS map (c, f) F EDS map.